Automatic Sequential Actuation of Multiple Cylinders in Mobile Cranes Using a Single Electro-Hydraulic Converter

Timofei Komarov , Victor Zhidchenko , and Heikki Handroos

LUT Mechanical Engineering, LUT University, Lappeenranta, Finland
E-mail: timofei.komarov@lut.fi, victor.zhidchenko@lut.fi, heikki.handroos@lut.fi

Abstract

The electrification of actuation systems of mobile cranes presents challenges in adaptating electro-hydraulic (EHA) or electro-mechanical (EMA) actuators. While the implementation of EHAs promises efficiency improvement, conventional hydrostatic systems require a dedicated electro-hydraulic energy converter (EHC) for each actuator. This study proposes a solution to actuate multiple actuators sequentially using a single EHC. The solution comprises two main parts: a hydraulic system featuring switching the connection between the EHC and the cylinders; and a control algorithm for automated crane movement. Performance was evaluated through simulation and compared with two conventional systems: one using a load-sensing system with proportional directional valves, and the other employing independent closed-loop circuits with a dedicated EHC for each cylinder.

Keywords: Automation, Mobile machines, Energy Efficiency, Electro-Hydraulics, Sequential Motion

1 Introduction

In recent decades, the development of mobile machinery has been focused on several key areas. One major area is automation, which is ongoing on several levels. Commercially available solutions pursue the increase of productivity and simplification of machine operation [1], while the remote operation remains in the research phase [2]. Automatic movement has been studied in both vehicle driving [3] and manipulator control [4]. However, the complexity and variability of the work environment remain to be the main challenge on the way to machine automation [5].

Another research direction is electrification of the machine powertrain, driven by the increase of energy efficiency and the reduction of carbon emissions [6]. The substitution of conventional valve-controlled hydraulics with electro-hydraulic actuators was found perspective for increasing energy efficiency of the mobile machines [7]. The common solution is to implement independent closed hydraulic circuits for each machine's actuator [8]. However, this approach requires an substantial number of electro-hydraulic actuators (5-8) for machine operation, posing significant challenges in implementation.

This article revises the approach to actuating multiple cylinders using a single electro-hydraulic converter (EHC) [9]. Previous research proposed switching between cylinders using fast on/off valves, and simulation demonstrated inconvenience of the solution for manual operation: every switch between cylinders caused high pressure oscillations.

To address this limitation, this study introduces path-planning, a switching algorithm, and automatic motion control. The system was evaluated using simulation and compared with a load-sensing system (LS-system) with proportional directional valves (DCVs) and a system with two independent EHC-based circuits.

2 Description of the System Under Study

A PATU655 mobile log crane is a hydraulic manipulator with a typical mechanical structure, presented in fig. 1. The crane comprises a pillar, a lift boom, and a jib (tilt) boom interconnected with rotational joints, and an extension boom connected to the jib by a linear joint.

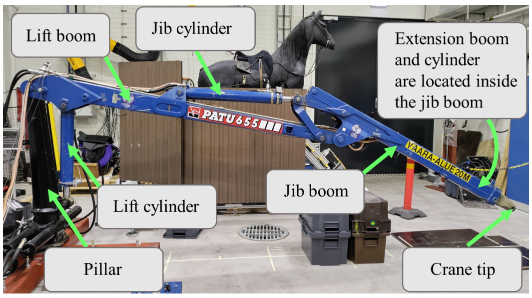

Figure 1: Mobile hydraulic log crane PATU 655, Laboratory of Intelligent Machines at LUT University, 2023 [10].

2.1 Electro-Hydraulic System Architecture

Figure 2 illustrates the proposed actuation system of a mobile log crane. System parameters are listed in tab. 1. The system's fluid power source is an EHC 1 comprising a Parker F11-019 pump [11] and a Parker GVM210-050 electric motor [12]. The crane actuators are hydraulic cylinders 3 and 4. Parker DS162CV on/off valves 2 [13] switch the connection between the EHC and the cylinders. The control system measures pressure in the cylinder chambers and EHC ports using pressure sensors 5. Pressure-relief valves 6 ensure overload protection for the system.

Operating an asymmetric cylinder with an EHC presents a challenge due to the need to compensate for differences in volumetric flow in cylinder chambers. Insufficient flow can cause cavitation, while excessive flow leads to a pressure rise. To address this issue, various solutions and system configurations have been studied [14]. In this research, a low-pressure line (LP-line) maintains a constant pressure of 5 bar by directing flow from the boost pump 8 or to the tank via a Parker DS163BN 3/2 directional control valve 7 [13].

Table 1: System parameters.

Parameter	Value
Lift cylinder piston diameter, mm	100
Lift cylinder rod diameter, mm	56
Lift cylinder stroke, mm	535
Tilt cylinder piston diameter, mm	90
Tilt cylinder rod diameter, mm	56
Tilt cylinder stroke, mm	780
Pump displacement, cm^3/rev	19

In the present research, only the movements of the lift and tilt cylinder are considered. However, the proposed system architecture can be expanded to a larger number of actuators.

3 Automatic Motion Algorithm

The automatic motion of a log crane is achieved through several steps:

1. Planning a path between the given start and end points considering crane kinematics limitations and obstacles within the discretized crane workspace.
2. Building a smooth trajectory along the obtained path.
3. Automatic movement of the hydraulic cylinders along the trajectory.

Considering movement of only the lift and tilt cylinders, the crane workspace is planar. However, the proposed automation approach can be expanded to spatial cases.

3.1 Path-planning Algorithm

A* path-planning algorithm provides a direct and simple solution for finding the shortest path in a weighted graph [15]. The implementation of this algorithm requires workspace discretization, and previous studies have used square cells in Cartesian coordinates to represent possible crane tip positions constrained by the crane kinematics [10].

However, linear tip movements in Cartesian coordinates require simultaneous control of both the lift and tilt booms, which is not possible with the proposed actuation system. To address this issue, the crane workspace was discretized with a step size 0.05 m using cylinder positions S1 and S2 instead of Cartesian coordinates (X,Z). The dependency between the tip position and the cylinder positions is determined by crane's geometry.

Constraining the A* algorithm to move only along coordinates S1 and S2 (excluding diagonal movements) allow crane operation using one cylinder at a time. Hence, the path-planning algorithm provides a sequence of cylinder movements to move between the given start and end points.

3.2 Trajectory Generation Algorithm

Cylinder trajectories are generated based on the sequence of cylinder motions provided by the A* path-planning algorithm. The crane movement consists of two successive phases: cylinder actuation and switching between active cylinders.

The trajectory of each cylinder is formulated using a jerk-bounded quintic polynomial method [16]. This approach ensures smooth trajectories between two given points with minimized movement duration, yet secures velocity, acceleration, and jerk constrains. The limits considered in this study are listed in the tab. 2.

Table 2: Actuators limits.

Parameter	Value
Lift cylinder maximum velocity, m/s	0.1
Lift cylinder maximum acceleration, m/s^2	0.2
Lift cylinder maximum jerk, m/s^3	0.2
Tilt cylinder maximum velocity, m/s	0.15
Tilt cylinder maximum acceleration, m/s^2	0.2
Tilt cylinder maximum jerk, m/s^3	0.2

Switching between cylinders can cause pressure oscillations in the system [9]. In static conditions, the pressure in cylinders is primarily determined by the applied load and depends on the crane configuration. Before switching, the pressure at the EHC ports equals to that of the previously operated cylinder. When the valves 2 open to connect the EHC to the next cylinder, the difference in pressure leads to uncontrolled flow through the valves, resulting in pressure oscillations.

To mitigate the problem, a switching algorithm has been de-

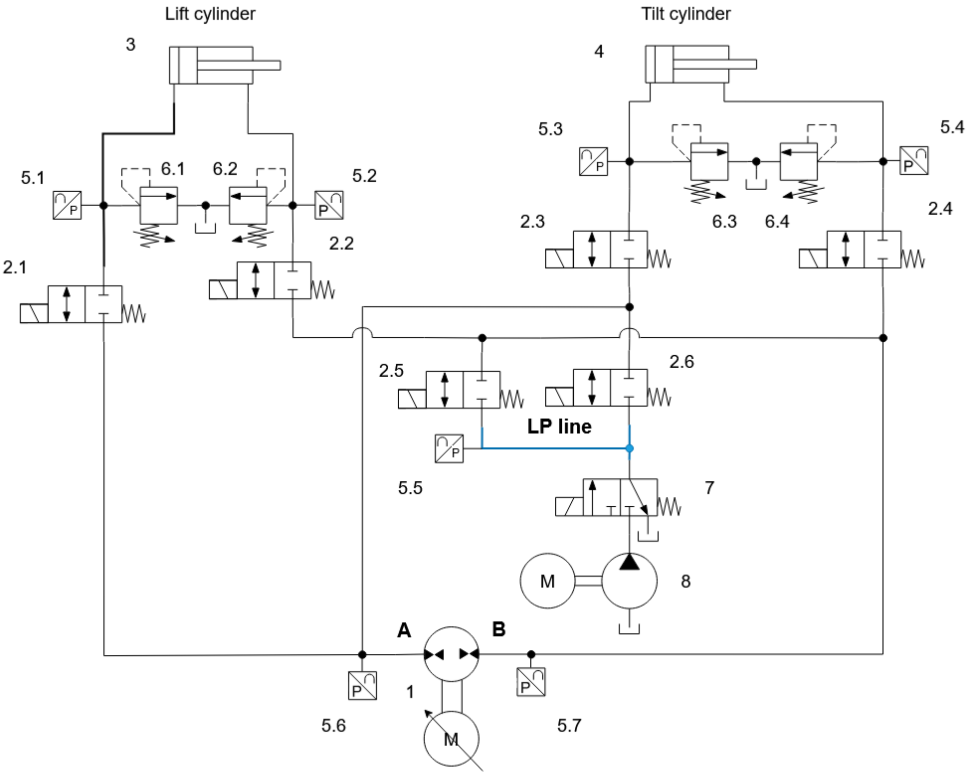

Figure 2: A diagram of the electrohydraulic actuation system featuring sequential control of multiple actuators using a single EHC

veloped. Firstly, the cylinders have to fully stop before switching. Secondly, a 0.5-second delay is introduced, when the EHC is temporarily disconnected from all cylinders.

During this pause, the algorithm identifies the chamber of the next cylinder with the load-holding pressure and sets it as the reference pressure for the corresponding EHC port. At the same time, the second EHC port is connected to the low-pressure line through valves 2.5 or 2.6 and to the low-pressure chamber of the next cylinder through valves 5.2, 5.3, or 5.4. After that, the EHC controls pressure at its ports to match that of the next cylinder. Once the pressure is stabilized, the corresponding on/off valves open, connecting the EHC and the cylinder.

Hence, the trajectory generation algorithm produces reference position, velocity, and acceleration of the cylinders, and regulates the switching order of the on/off valves.

3.3 Movement Control Algorithm

Cylinder movement control is based on the Virtual Decomposition Control (VDC) approach, which calculates the actuator forces needed to achieve the required motion by calculating the manipulator dynamics [17]. This versatile algorithm has been successfully implemented in hydraulic manipulators, demonstrating high accuracy [4].

The reference rotation velocity of the EHC, ω_{ref}, is calculated based on the required pump volumetric flow Q_{ref} and closed-loop proportional force and velocity control:

$$\omega_{ref} = \frac{Q_{ref}}{V_P} + k_F \cdot (F_r - F_{meas}) + k_v \cdot (v_{ref} - v_{meas}) \tag{1}$$

where V_P is a pump displacement, m^3/rev; F_r and F_{meas} are actuator reference and measured forces, respectively, N; v_{ref} and v_{meas} are cylinder reference and measured velocities, respectively, m/s; and k_F and k_v are proportional coefficients for feedback force and velocity control, manually tuned for suitable performance.

The required pump volumetric flow rate Q_{ref} is determined using the dynamic continuity equation:

$$Q_{ref} = \begin{cases} \frac{\dot{F}_r \cdot x_{meas}}{B_e} + A_A \cdot v_{ref}, & \text{if } G > 0 \\ \frac{\dot{F}_r \cdot (x_{max} - x_{meas})}{B_e} + A_B \cdot v_{ref}, & \text{otherwise} \end{cases} \tag{2}$$

where B_e is the effective bulk modulus of oil in a chamber, Pa; x_{max} is a cylinder stroke, m; and A_A and A_B are piston-side and rod-side cylinder areas, respectively, m^2; $G \in -1, 1$ corresponds to the direction of the gravity force estimated from the crane position and determines the cylinder chamber with the load-holding pressure. For the lift cylinder, G is not calculated because of its unidirectional load.

The force balance equation is used to estimate the generated cylinder force F_{meas}:

$$F_{meas} = p_A \cdot A_A - p_B \cdot A_B - k_V \cdot v_{ref} \tag{3}$$

where p_A and p_B are the pressures in the piston-side and rod-side cylinder chambers, respectively, Pa; and k_V is the coefficient of cylinder viscous friction, N/(m/s).

The control system coefficients were found empirically and are listed in the tab. 3.

Table 3: Control system parameters.

Parameter	Value
Lift cylinder k_F	$2 \cdot 10^{-5}$
Lift cylinder k_v	10
Tilt cylinder k_F if $G \geq 0$	$2 \cdot 10^{-5}$
Tilt cylinder k_v if $G \geq 0$	10
Tilt cylinder k_F if $G < 0$	$-1 \cdot 10^{-5}$
Tilt cylinder k_v if $G < 0$	10

4 Simulation

The system performance was analyzed using a simulation in MATLAB/Simulink. The multibody dynamics of the crane was modeled using an iterative Newton-Euler dynamic formulation [18] and verified against the physical crane at LUT University (fig. 1). Since the reference crane is not equipped with a grapple, load swing was not considered, and logs were not explicitly modeled. Instead, a point mass of 180 kg, attached to the crane tip, represented the payload of a single log.

The electro-hydraulic system model incorporates the crane cylinders, the EHC, and on/off valves. The cylinder models neglect the leakages but include a friction model developed in previous research [18]. The EHC model accounts for the first-order dynamics of the electric motor, with a 50 ms rise time, and incorporates a laminar pump leakage model based on the manufacturer data [11]. Estimation of consumed power comprises the calculation of mechanical energy delivered to the pump and accounts for the motor efficiency based on the charts from the datasheet [12]. The on/off valves are modeled using the first-order dynamics and flow characteristics derived form the datasheet [13].

Pressure-relief valves were excluded, as system operation during overload conditions is not considered in this study. To avoid unnecessary model complexity, the LP-line, boost-pump, and 3/2 valve were simplified to a constant pressure source of 5 bar.

The Simulink model incorporates the previously described movement control algorithm and valve-switching logic. Path-planning and trajectory-building algorithms are implemented in MATLAB script.

4.1 Reference Systems

The proposed electro-hydraulic system is compared with two state of the art approaches: an LS-system with DCVs; and a system with an independent EHC for each cylinder. The implementation of the modified A* algorithm for both reference systems to find the shortest path was investigated in a previous study [10]. The movement velocity was adjusted to limit the cycle duration to 11-13 seconds, which represents typical operator performance [19].

4.1.1 LS-system with DCVs

Figure 3 illustrates the hydraulic diagram of the LS-system with DCVs. It uses the same EHC 1 for power supply as in the proposed electro-hydraulic system. The DCVs 4 are Bosch Rexroth 4WRPEH 6 with a rated flow of 40 lpm [20].

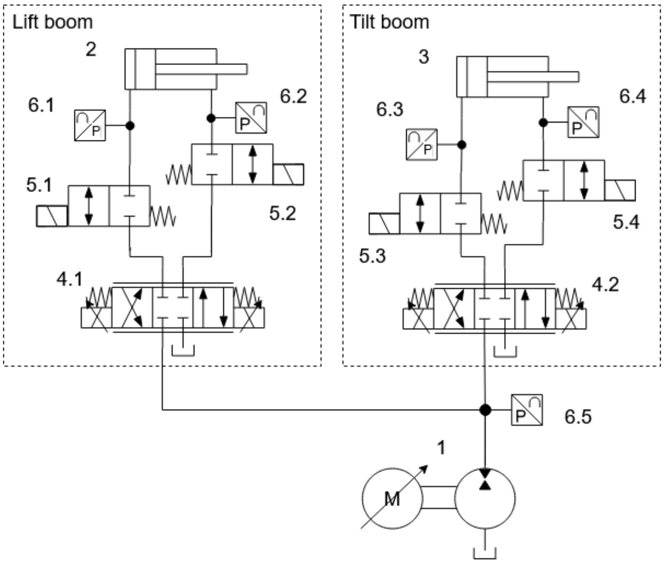

Figure 3: Hydraulic diagram of the LS-system with DCVs

The LS-system maintains the supply pressure at a level greater than the highest pressure in the cylinders by a predefined offset, commonly of 35 bar. Conventionally, this function is controlled hydro-mechanically with a variable-displacement LS-pump [21]. However, in this system, pressure regulation is performed by adjusting the EHC's rotation velocity based on real-time cylinder pressures measured by pressure sensors 6.1-6.4.

An open-loop model-based control is implemented to calculate the EHC reference rotation velocity ω_{ref}:

$$\omega_{ref} = (p_{LS} + \Delta p_{LS} - p_{max}) \cdot k_{LS} + \frac{v_{lift} \cdot A_{lift} + v_{tilt} \cdot A_{tilt}}{V_P} \quad (4)$$

where p_{LS} is the measured supply line pressure, Pa; Δp_{LS} is the pressure offset, Pa; p_{max} is the maximum cylinder pressure, Pa; $k_{LS} = 5$ is a proportional feedback coefficient; A_{lift} and A_{tilt} are cylinder areas depending on the movement direction, m^2.

The cylinder motion control combines three components: an open-loop model-based control U_{MB}; a closed-loop proportional position control; and a closed-loop PD velocity control:

$$U_{DCV} = k_x \cdot (x_{ref} - x_{meas}) + k_{vP} \cdot (v_{ref} - v_{meas}) + k_{vD} \cdot \frac{\mathrm{d}(v_{ref} - v_{meas})}{\mathrm{dt}} + U_{MB} \quad (5)$$

where U_{DCV} is the DCV control voltage, V; $k_x = 30$ is a closed-loop position proportional coefficient; $k_{vP} = 20$ and $k_{vD} = 10$ are closed-loop PD velocity control coefficients.

The model-based control component U_{MB} is defined as:

$$U_{MB} = \frac{Q}{C_V \cdot \sqrt{p_{LS} - p}} \quad (6)$$

where $Q = \dot{x}_{ref} \cdot A$ is the volume flow rate required to achieve the reference cylinder velocity $\dot{x}_{ref}$, m^3/s; and C_V is a valve flow coefficient.

4.1.2 System with independent EHCs

A reference closed-loop circuit with an independent EHC for each cylinder is presented in fig. 4. The illustrated system controls a single cylinder, so the considered crane requires two such systems to actuate lift and tilt cylinders. The model of the system and the control algorithm were developed in the previous research [22]. The on/off valves 5.1 and 5.2 were not modeled because this research does not consider system behavior during overloading conditions.

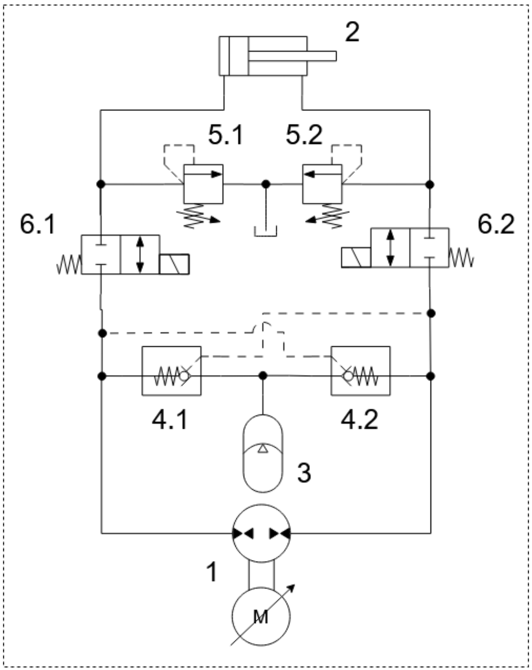

Figure 4: Diagram of the hydraulic system with independent EHCs [22]

4.2 Simulation Conditions

The simulations replicated typical log crane operations: logs loading from the pile into the trailer, and unloading them to the ground. Figure 5 illustrates the crane, an obstacle, and start and end points considered in the simulation. The logs are supposed to be grabbed close to their center of mass for ensuring the balance. Therefore, the brown circles describe positions of the centers of mass of the logs, even though normally the logs are pointed orthogonally to the road. The simulation conditions included a vertical obstacle representing the log trailer bunks.

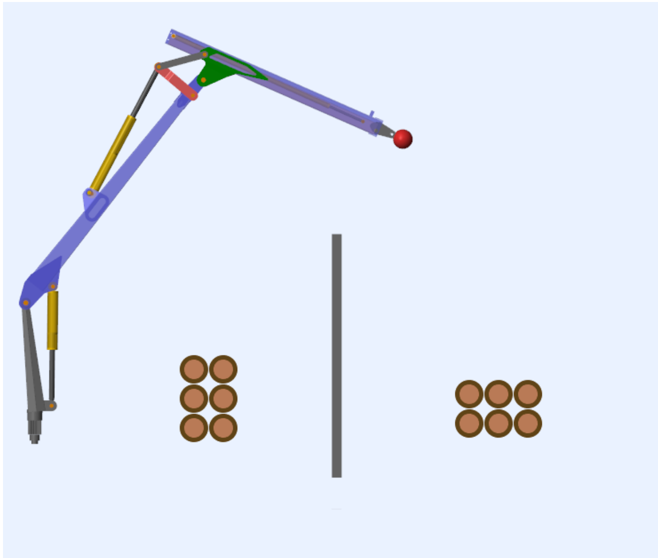

Figure 5: Diagram of the simulated working environment. The gray vertical line represents the obstacle, and brown circles depict log positions

The set of points included 6 positions in the pile and 6 positions in the truck, resulting in 36 combinations of start and end points. For each combination of the points, two shortest paths were found: one with the proposed electro-hydraulic system, and one with reference systems.

5 Results

Figure 6 presents a boxplot comparing the ratio of total energy consumption per cycle during a single simulation of the proposed system (E) to that of the LS-system with DCVs (E^{DCV}) and the system with independent EHCs (E^{EHC}). Summary statics is presented in the tab. 4.

Table 4: Summary statistics of the ratio of total energy consumption per cycle of the proposed system (E) compared to the LS-system with DCVs (E^{DCV}) and the system with independent EHCs (E^{EHC}).

Parameters		$\frac{E}{E^{DCV}}$	$\frac{E}{E^{EHC}}$
Loading logs	75th percentile	31.38 %	75.10 %
	Median	28.33 %	68.50 %
	25th percentile	26.10 %	61.98 %
Unloading logs	75th percentile	35.55 %	48.87 %
	Median	32.37 %	42.10 %
	25th percentile	25.31 %	32.74 %

Figure 7 illustrates the boxplot of a ratio of cycle durations

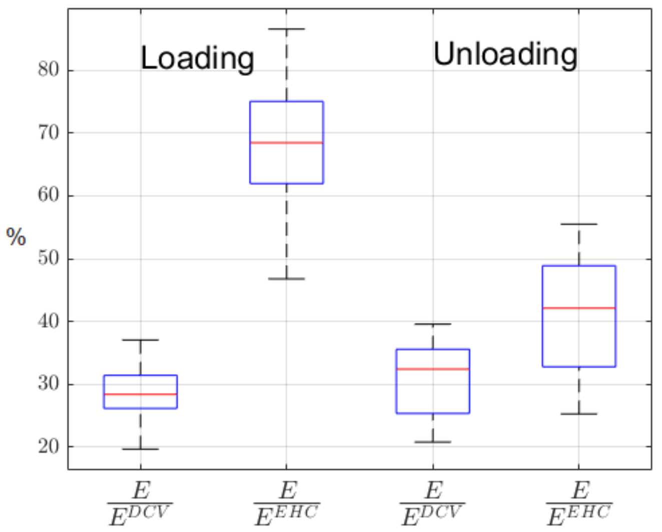

Figure 6: Ratio of total energy consumption per cycle of the proposed system (E) to that of the LS-system with DCVs (E^{DCV}) and the system with independent EHCs (E^{EHC})

during operation of the proposed system (T) to those of the LS-system with DCVs (T^{DCV}) and the system with independent EHCs (T^{EHC}). Table 5 contains the corresponding summary statistics.

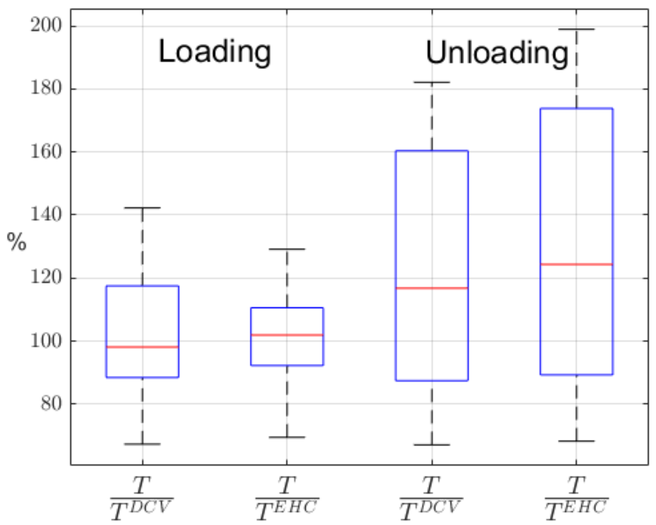

Figure 7: Ratio of cycle durations of the proposed system (T) to those of the LS-system with DCVs (T^{DCV}) and the system with independent EHC (T^{EHC})

An example of the shortest paths found during a simulation is presented at fig. 8. The green and pink circles illustrate the start and final points, respectively, and the green lines represent the starting crane configuration. The trajectory building algorithm transforms the paths into reference commands for actuation systems. Figure 9 demonstrates reference trajectories and actual crane tip positions obtained in a simulation for each actuation system.

Table 5: Summary statistics values of the ratio of cycle durations of the proposed system (E) to those of the LS-system with DCVs (E^{DCV}) and the system with independent EHCs (E^{EHC}).

Parameters		$\frac{T}{T^{DCV}}$	$\frac{T}{T^{EHC}}$
Loading logs	75th percentile	117.50 %	110.57 %
	Median	98.11 %	101.90 %
	25th percentile	88.41 %	92.21 %
Unloading logs	75th percentile	160.37 %	173.78 %
	Median	116.75 %	124.31 %
	25th percentile	87.43 %	89.27 %

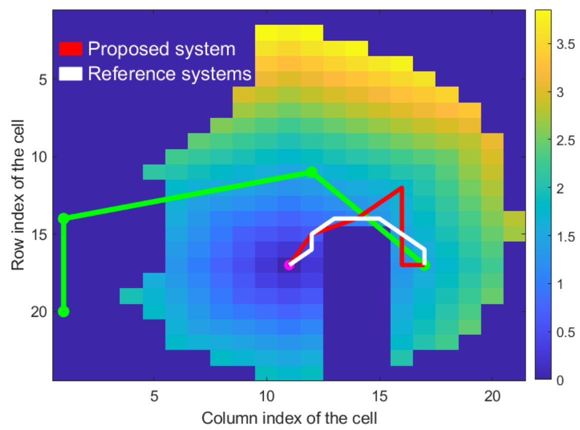

Figure 8: An example of the paths found by the developed path-planning algorithm for the proposed and reference systems

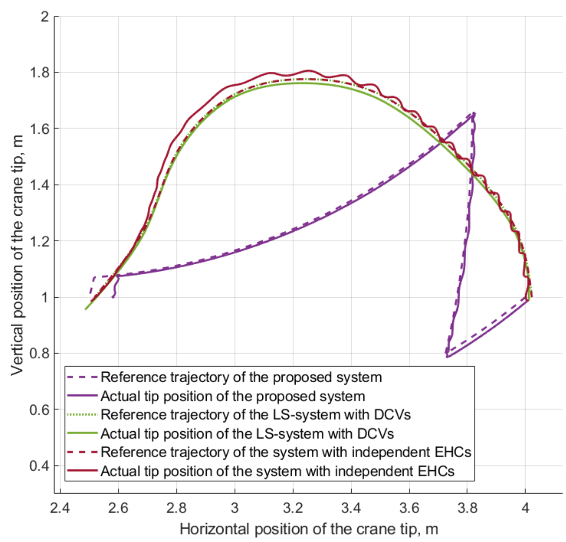

Figure 9: Trajectories generated based on the found paths, and actual crane tip movements when following them

Conclusion

A solution featuring a single EHC for the automatic sequential control of hydraulic cylinders in the log crane was developed in this study. Simulations demonstrated significant reduction in energy consumption with median values reaching 28.33 % and 68.50 % for log loading cycles and 32.37 % and 42.10 % for log unloading cycles compared to the reference LS-system with DCVs and the system with independent EHCs, respectively.

The decrease in energy consumption was achieved due to two key factors. First, controlling only a single actuator at a time simplifies trajectory building and cylinder position control, allowing the EHC to operate in its high-efficiency range. Second, when cylinders are disconnected, they don't consume energy for load holding, unlike systems using DCVs or independent EHCs.

The cycle durations of the proposed system were close to ones of the reference systems during log loading cycles. However, during unloading, the cycle time increased, with median values reaching 116.75 % and 124.31 % compared to the LS-system with DCVs and the system with independent EHCs, respectively. Moreover, the 75th percentile of the duration ratio reached 160.37 % and 173.78 % relative to the reference systems. This significant cycle slowdown is primarily attributed to the high correlation between the number of switches between the cylinders and cycle duration. Every switch introduces a fixed 0.5 s delay for pressure stabilization, and since the cylinders have to stop for switching, movement speed is reduced due to additional acceleration and deceleration phases.

The proposed system provides a wide range of opportunities for further study. First, optimizing the path-planning algorithm to minimize switches between the cylinders could improve work cycle duration. Second, the approach of actuating multiple cylinders with the fewest possible EHCs allows for a wide variety of potential modifications and combinations within actuation systems. Third, incorporating the extension boom introduces redundancy, which can be used for energy efficiency improvement and control optimization. Finally, further investigation into the implementation of the VDC in EHC-based systems is needed for maximizing the system performance and accuracy.

References

[1] The perfect cut. ctl - the cut-to-length method. Ponsse Plc, Ponssentie 22, 74200 Vieremä, 2023.

[2] Aamir Mahmood, Sarder Fakhrul Abedin, Mattias O'Nils, Mats Bergman, and Mikael Gidlund. Remotetimber: An outlook for teleoperated forestry with first 5g measurements. *IEEE Industrial Electronics Magazine*, 17(3):42–53, 2023.

[3] Jouko Kalmari, Juha Backman, and Arto Visala. Coordinated motion of a hydraulic forestry crane and a vehicle using nonlinear model predictive control. *Computers and Electronics in Agriculture*, 133:119–127, 2017.

[4] Janne Koivumäki and Jouni Mattila. High performance nonlinear motion/force controller design for redundant hydraulic construction crane automation. *Automation in Construction*, 51:59–77, 2015.

[5] Volker Waurich, Benjamin Beck, Jürgen Weber, and Frank Will. Levels of digitalization for construction machinery on the connected and automated construction site. In Johannes Fottner, Konrad Nübel, and Dominik Matt, editors, *Construction Logistics, Equipment, and Robotics*, pages 157–165, Cham, 2024. Springer Nature Switzerland.

[6] Antti Lajunen, Panu Sainio, Lasse Laurila, Jenni Pippuri-Mäkeläinen, and Kari Tammi. Overview of powertrain electrification and future scenarios for non-road mobile machinery. *Energies*, 11(5), 2018.

[7] T. A. Minav, C. Bonato, P. Sainio, and M. Pietola. Efficiency of direct driven hydraulic drive for non-road mobile working machines. In *2014 International Conference on Electrical Machines (ICEM)*, pages 2431–2435, 2014.

[8] Daniel Hagen, Damiano Padovani, and Morten K. Ebbesen. Study of a self-contained electro-hydraulic cylinder drive. In *2018 Global Fluid Power Society PhD Symposium (GFPS)*, pages 1–7, 2018.

[9] Teshale Bekele, Rafael Åman, and Heikki Handroos. The control of multiple actuators using single iehec pump/motor. In *10th International Fluid Power Conference (10. IFK)*, 03 2016.

[10] Victor Zhidchenko, Timofei Komarov, Antoine Williot, Nathan Bauer, and Heikki Handroos. A method for planning the trajectory of mobile hydraulic crane booms with a focus on energy efficiency. In *2023 IEEE 21st International Conference on Industrial Informatics (INDIN)*, pages 1–7, 2023.

[11] Parker Hannifin, Mobile Controls Division. *Catalogue HY17-8249/US - Hydraulic Motor/Pump Series F11/F12*, 2004.

[12] Parker Hannifin, Hydraulic Pump and Power Systems. *GVM Global Vehicle Motor Power Series. Permanent Magnet (PMAC) Motor for Mobile Systems*, 2022.

[13] Parker Hannifin, Hydraulic Valve Division. *Catalog 3105/USA. Directional Control Valves. Series DS162*.

[14] Zhongyi Quan, Long Quan, and Jinman Zhang. Review of energy efficient direct pump controlled cylinder electro-hydraulic technology. *Renewable and Sustainable Energy Reviews*, 35:336–346, 2014.

[15] Peter E. Hart, Nils J. Nilsson, and Bertram Raphael. A formal basis for the heuristic determination of minimum cost paths. *IEEE Transactions on Systems Science and Cybernetics*, 4(2):100–107, 1968.

[16] Sonja Macfarlane and Elizabeth Croft. Jerk-bounded manipulator trajectory planning: Design for real-time applications. *Robotics and Automation, IEEE Transactions on*, 19:42 – 52, 03 2003.

[17] Wen-Hong Zhu. *Virtual decomposition control: toward hyper degrees of freedom robots*, volume 60. Springer Science & Business Media, 2010.

[18] Iuliia Malysheva, Heikki Handroos, Victor Zhidchenko, and Alexander Kovartsev. Faster than real-time simulation of a hydraulically actuated log crane. In *2018 Global Fluid Power Society PhD Symposium (GFPS)*, pages 1–6, 2018.

[19] Pedro La Hera and Daniel Ortiz Morales. What do we observe when we equip a forestry crane with motion sensors? *Croat. J. For. Eng.*, 40(2):259–280, August 2019.

[20] Bosch Rexroth AG. *RE 29121*, 2022.

[21] Henrik Pedersen, Torben Andersen, and Michael Hansen. Load sensing systems - a review of the research contributions throughout the last decades. In *Proceedings 4th IFK Workshop*, pages 125–139, 01 2004.

[22] Timofei Komarov, Victor Zhidchenko, and Heikki Handroos. Effect of electrification on the energy efficiency of boom trajectories of semi-autonomous mobile cranes. In *Advancements in Fluid Power Technology: Sustainability, Electrification, and Digitalization*, 08 2024.